A Simple and Compact Dual-Band BPF with High Frequency Ratio to Support Microwave and Millimeter-Wave Applications

Ahmed Lateef Khudaraham[1], Dhirgham Kamal Naji[2]
Electonic and Communication Engineering Department, College of Engineering,
Al-Nahrain University, Baghdad, Iraq

Abstract— To fulfill the simulation requirements for the fast progress of wireless communication systems, the cohabitation of microwave and millimeter-wave technologies becomes very trendy. This paper represents a dual-band BPF by using parallel coupled microstrip lines and inserting multi-stubs to enhance the overall filter performance. The proposed filter can operate at microwave and millimeter-wave frequencies simultaneously. Good performance is revealed in this filter in terms of insertion and return losses with ultra-wide stopband between the two passbands. The proposed filter is simulated with CST microwave studio package on a Rogers RT6002 substrate. The center frequencies achieved are at 5.85 GHz and 30 GHz with frequency ratio of 5.13 and fractional bandwidths (FBW) of 42.6% and 3.6% respectively. The proposed BPF can be used in WLAN and 5G communication systems applications.

Index Terms— Bandpass filter (BPF), Microwave, Millimeter-wave, fractional bandwidth (FBW), dual-band, passband, WLAN, DGS.

1 Introduction

The wireless communication systems today use the microwave bands for most of the applications. The ascending growth of data transfer and technologies demand a multi-gigabit connections which can be achieved through moving towards the millimeter-wave spectrum. The high frequency ratio is a major principle in granting such filters. Most of the previous BPFs can provide frequency ratio lower than 4. Alternatively, the dual-band operation was granted by cascading a broadband bandpass filter with a stopband but this method suffered from large circuit size in increased insertion loss [1]. A multimode resonators can be utilized by loading stubs to different resonators such as stepped impedance resonator (SIR) [2], [3], open loop resonator [4], [5], ring resonator [6]. In general, stepped-impedance resonators and T-shaped line have been utilized to design a compact dual-band BPF that can operate at microwave spectrum only at 2.47 GHz and 5.37 GHz with 25% and 15.1% of fractional bandwidths respectively [7]. The filter in [8] uses a ring resonator with coupled microstrip lines to design a dual-band operation BPF centered at 2.3 GHz and 4.3 GHz. A compact microstrip resonant cell has been introduced in [9] to design dual-band BPF centered at 3.75 GHz and 5.45 GHz with fractional bandwidths of 10.7% and 7.3% respectively. A quadruple mode square resonator is presented in [10] with dual-band operation centered at 2.45 GHz (18% FBW) and 5.2 GHz (4.8% FBW). In [11], a compact dual-band BPF is designed operating at 0.61 GHz (32.3% FBW) and 1.36 GHz (10.5% FBW) by using coupled three-section stepped-impedance resonator with two reflecting zeros and five out-of-band transmission zeros (TZs). The filter in [12] operates at dual-band operation centered at 1.57 GHz (9% FBW) and 2.45 GHz (8.5% FBW), this filter is designed by utilizing a quad mode symmetrical resonator consisting of a pair of coupled lines and transmission line sections. A coupled SIR is used with embedded resonators to design a dual-band BPF centered at 2.49 GHz (15.6% FBW) and 3.49 (8% FBW) with sharp suppression to the harmonics due to the generation of multiple transmission zeroes [13]. In [14], a dual-wide band BPF is presented centered at 2.96 GHz (27.7%FBW)) and 5.695 GHz (23.4%FBW) by using quadruple mode resonator with wide stopband. All of the aforementioned filters were designed to operate at microwave spectrum with frequency ratio below 4 which is not suitable to jump from microwave spectrum to millimeter-wave spectrum. The most ratio achieved is in [15] with a wide stopband from microwave to millimeter-wave region. The ratio was 12.59 with two passbands centered at 2.37 GHz (19.41%FBW) and 29.84 GHz (6.5%FBW). The main drawback with this filter is in its high complexity since multi-layers and different techniques and material have been used.

In this paper, a simple, compact, and effective design of dual-band BPF is proposed with large frequency ratio. Good performance has been achieved with high %FBW for each band. The stopband between the two passbands has been enhanced by the introduction of DGS structure. Design stages, results, and parametric studies are illustrated.

2 Design Concept

In this section, the steps and evolution of the design are detailed step by step from the initial BPF to the proposed and optimized BPF. The aim of these steps is to generate a dual-band response operated at 5.85 GHz and 30 GHz with maximum simplicity and good performance. Each step will be described individually from the initial coupled lines with inverted T-resonator to the addition of multi-stubs that provided the second passband and performance enhancement.

2.1 Filter Geometry

The final geometry of the proposed BPF is shown in Fig.1. The

proposed filter is comprised of parallel coupled lines with two parallel T-lines opposite to each other at the center of the filter with two stubs attached to both ends of the coupled lines. The overall dimensions of the BPF (Lsub x Wsub) is 10 x 20 mm2 and its simulated using CST-MW studio on a Rogers TR6002 substrate with thickness of 0.127 mm, dielectric constant 2.94. A two ports of 50 ohms are used for transmission of the signal for input and output. Two coupled transmission lines (L1 x W1) are connected to the ports. Another line is coupled to the previous lines separated by a gap (g1) along the horizontal section of the proposed BPF with dimensions (L2 x W2). Two T-shaped lines are placed oppositely parallel to each other along the horizontal line at the center of the filter with dimensions defined as (L4 x W4 and L5 x W5) for the upper T-line and (L3 x W3 and L6 x W6) for the lower T-line. The two attached stubs at the coupled lines of the ports are defined as (L7 x W7). Finally, a slot in at the ground surface of the filter is proposed (L8 x W8) in order to enhance the overall filter performance. Table (1) lists the optimized dimensions of the proposed filter.

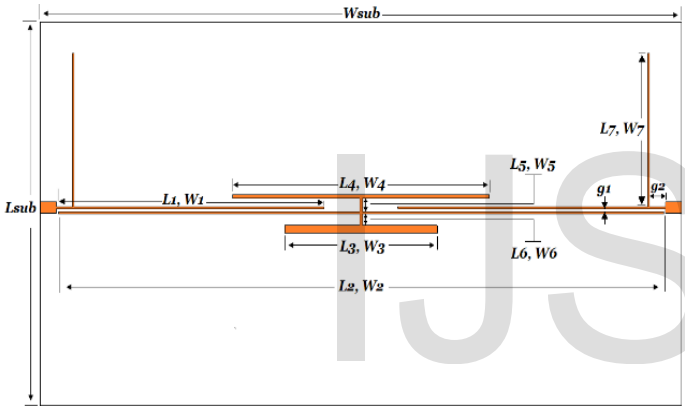

(a)

(b)

Fig.1. Full structure of the proposed BPF: (a) front view; (b) back view.

TABLE 1

GEOMETRIC DIMENSIONS OF THE OPTIMIZED PROPOSED BPF.

Parameter	Value mm	Parameter	Value mm
Lsub	10	*W1*	0.06
Wsub	20	*W2*	0.06
L1	8.35	*W3*	0.2
L2	18.86	*W4*	0.1
L3	4.75	*W5*	0.1
L4	8.0	*W6*	0.1
L5	0.34	*W7*	0.06
L6	0.3	*W8*	0.5
L7	4.0	*g1*	0.06
L8	2.0	*g2*	0.5

(a)

2.2 Design Stages

Fig.2 demonstrates the procedure for the three design stages applied to design the proposed BPF, namely:

Stage-1 (BPF 1): A single-band BPF is designed that can operate at microwave spectrum by initiating two simple parallel lines with a centered inverted T-shaped line as illustrated in Fig.2 (a). The cutoff frequency of this filter is centered at 6.75 GHz with -0.3 dB and -12 dB of insertion and return losses respectively at the center frequency as illustrated in Fig.3 (a). As can be seen, a wide stopband has been granted up to millimeter-wave region but with some ripples that can be eliminated in the next steps.

Stage-2 (BPF 2): The second passband is generated by adding another T-shaped line in the center as presented in Fig.2 (b) resulting in a 30.35 GHz passband. At this point, BPF2 is operating at dual-bands centered at 6.2 GHz with insertion and return losses of -0.19 dB and -14 dB respectively, and 30.35 GHz with -1.1 dB insertion loss and -8 dB return loss as shown in Fig.3 (b). It is obvious that the filter is suffering from high reflections and unwanted frequencies that should be removed in the next steps to enhance overall filter performance.

Stage-3 (BPF 3): The ultra-wide rejection band that must be achieved to jump from microwave to millimeter-wave spectrum is considered as a major challenge particularly with the simple single-layered design. As observed, the response of BPF2 in not as anticipated in terms of insertion loss, return loss and overall characteristics. Inserting two symmetrical stubs to the coupled lines as shown in Fig.2 (c) have enhanced the overall performance and the two passbands have been sharper in the in-band out-band regions with less reflections as compared to BPF2. The response of this filter is illustrated in Fig.3 (c).

At this stage, both passbands have been enhanced, the first passband operates with dual modes and centered at 5.78 GHz (4.57 GHz-GHz) with 3-dB fractional bandwidth of 42.2% and -0.6 dB and -9 dB of insertion and return losses respectively at the center frequency with two poles at 5 GHz (-51 dB) and 6.3 GHz (-46.6 dB). The second passband is centered at 29.9 GHz (29.6 GHz-30.3 GHz) with insertion and return losses of -0.5 dB and -30.3 dB respectively at the center frequency.

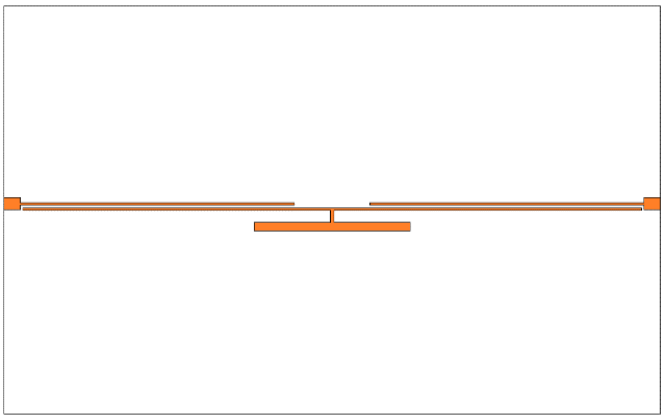

(b)

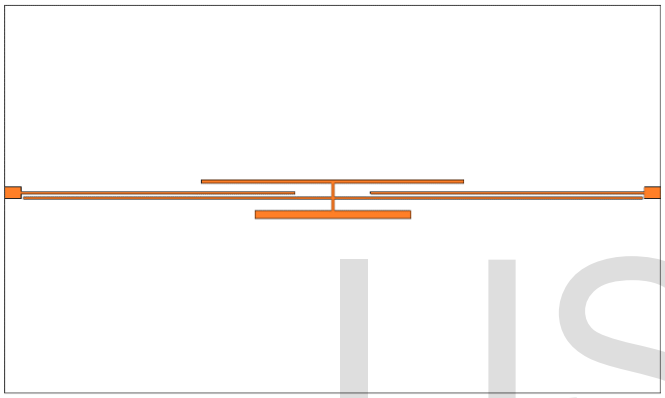

(c)

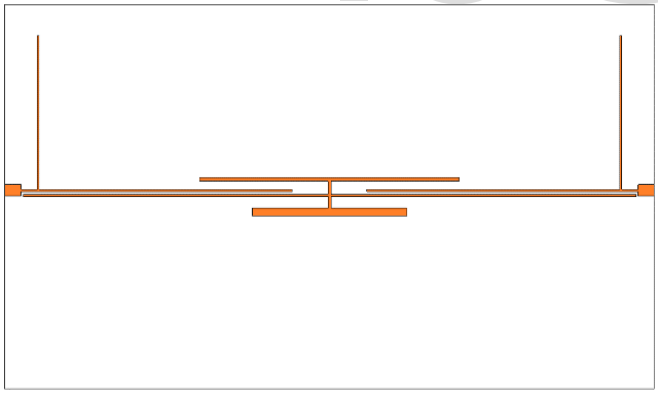

Fig.2. Geometry of various filters involved in the design evolution process: (a) BPF1; (b) BPF2; (c) BPF3

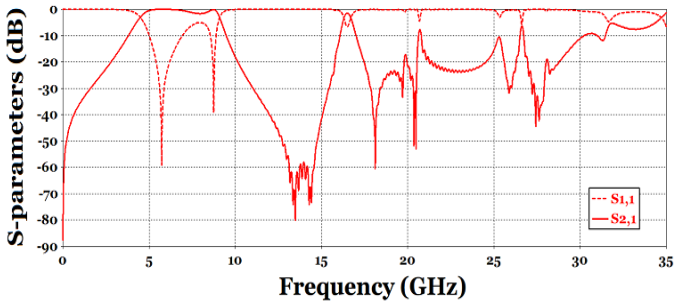

(a)

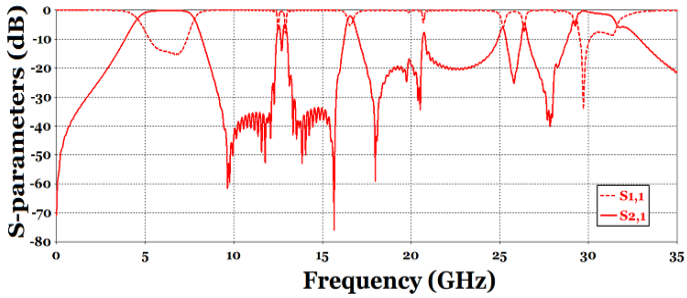

(b)

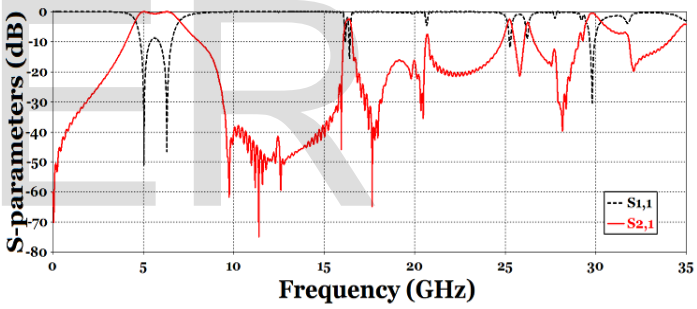

(c)

Fig.3. S-parameters of: (a) BPF1; (b) BPF2; (c) BPF3

2.3 Optimized Proposed BPF

More improvements should take place in order to suppress the harmonics in between the two passbands to further enhance the stopband. In order to optimize the performance of the proposed filter, the principles of the Defected Ground Structure (DGS) is applied upon the ground part of the proposed filter. Due to this application, both passbands have been optimized and all of the unwanted harmonics have been disposed. The final structure of the optimized proposed filter with the ground layer is shown in Fig.4.

As a finishing results, the filter has been optimized in order to present the best characteristics with the proposed structure. The final circuit size is 20x10 mm² and highlighted with compact size and simple scheme. Fig.5 shows the response of the optimized proposed BPF. The first passband is centered at 5.85 GHz (4.6 GHz-7.1 GHz) with dual modes for WLAN applications

- *Ahmed Lateef Khudaraham is currently pursuing masters degree program in electrictronics and communications engineering in Al-Nahrain University, Iraq, PH-(+9647815900950). E-mail: ahmed.lateef771@gmail.com*
- *Dhirgham Kamal Naji is currently a Asst. Prof. in electrictronics and communications engineering in Al-Nahrain University, Iraq, PH-(+9647721678992). E-mail: dknaji@yahoo.com*
(*This information is optional; change it according to your need.)*

with a 3-dB FBW of 42.7 %, with insertion and return losses of -0.2 dB and -12.7 dB respectively at the center frequency. The two poles of the first passband that caused the dual-mode operation are located at 5.3 GHz (-50 dB) and 6.3 GHz (-35.7 dB). The ultra-wide stopband started from 7.1 GHz to 29.5 GHz hopping from microwave spectrum to millimeter-wave spectrum. The second passband is centered at 30 GHz for 5G and high speed satellite transmission applications (29.5 GHz-30.6 GHz) with a 3-dB FBW of 3.6 % and -0.4 dB insertion loss and -52.3 dB return loss at the center frequency. The frequency ratio between the two passbands is 5.13 witch is the ratio between the center frequencies of the second passband to the center frequency of the first passband.

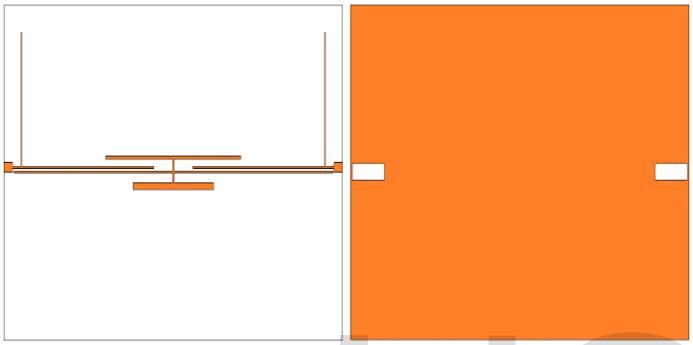

(a) (b)

Fig.4. Optimized proposed BPF: (a) front view; (b) back view.

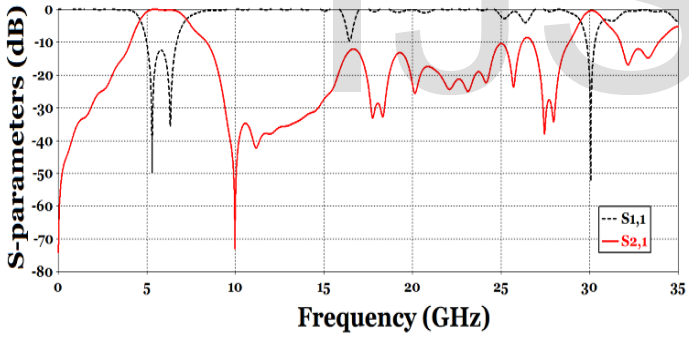

Fig.5. S-parameters of optimized proposed BPF.

3 Paramertic Study

Parametric studies have been encountered in order to characterize the parameter's effects of the proposed BPF. The performance of the filter is largely effected by varying ***L3***, ***L5***, ***L6*** and ***L7***. Each of these parameters are discussed and their effects are monitored on the response of the filter.

I. Effect of *L3*

The effect of this parameter is notified at both passbands but mainly on the second passband as revealed in Fig.6. The center frequency of the 2nd passband is shifted to various points by the changing of the value of the parameter, as well as the 1st passband also a slight shifting is visualized by this change.

II. Effect of *L5*

Both passbands are shifted to lower cutoff frequency by increasing the value of ***L3***. The effect is shown in Fig.7.

III. Effect of *L6*

The independent control of the 1st passband can be reached by the observing the effect of this parameter as shown in Fig.8. The 1st passband is mainly effected by changing of this parameter and shifting can be notified to multiple cutoff frequencies, whereas the 2nd passband almost stayed the same.

IV. Effect of *L7*

Also the 2nd passband can be tuned independently by varying L7 as presented in Fig.9. The shifting of the 2nd passband to lower or higher frequency can be observed by changing this parameter, however the 1st passband is effected only in its return loss.

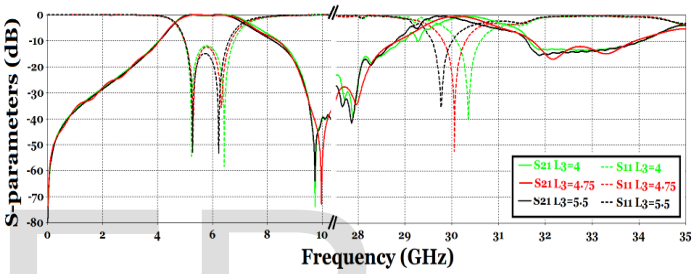

Fig.6. Effect of varying L3.

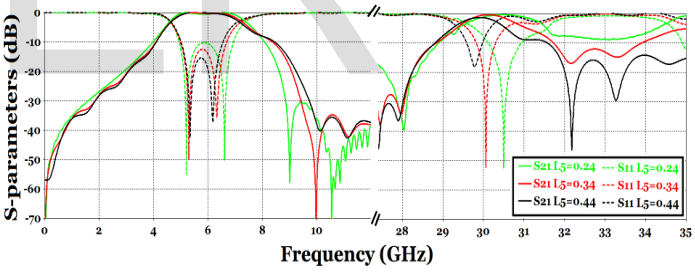

Fig.7. Effect of varying L5.

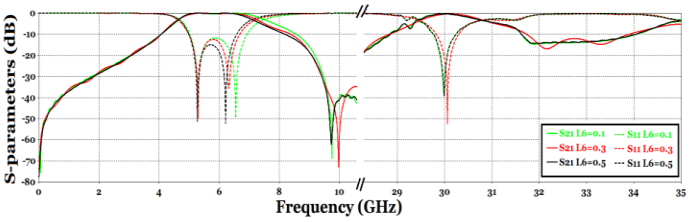

Fig.8. Effect of varying L6.

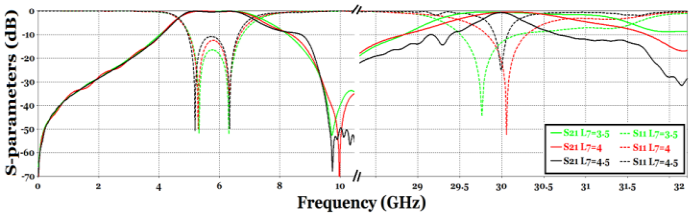

Fig.9. Effect of varying L7.

As a summary for the parametric study, Table (2) sorts each parameter with its related values and their effect on the center frequency, insertion loss and return loss in order to achieve a richer view and understand to the effect of each parameter.

TABLE 2
SUMMARY FOR THE EFFECT OF THE PROPOSED FILTER'S PARAMETERS.

Parameter	*Value (mm)*	*f01 (GHz)*	*f02 (GHz)*	*IL1 (dB)*	*RL1 (dB)*	*IL2 (dB)*	*RL2 (dB)*
L3	4	5.9	30.4	0.4	12.5	0.4	40
	4.75	5.85	30	0.2	12.7	0.4	52.3
	5.5	5.78	29.6	0.4	13	0.5	36
L5	0.24	5.9	34.2	0.3	10	0.5	22
	0.34	5.85	30	0.2	12.7	0.4	52.3
	0.44	5.7	28.7	0.5	12.9	0.5	29
L6	0.1	5.95	30	0.2	12.6	0.4	39
	0.3	5.85	30	0.2	12.7	0.4	52.3
	0.5	5.7	30	0.2	13	0.4	39
L7	3.5	5.85	29.7	0.2	11	0.3	30
	4	5.85	30	0.2	12.7	0.4	52.3
	4.5	5.85	29.9	0.2	16	0.4	25

4 SURFACE CURRENT DISTRIBUTION

Simulation results of the current distribution on the surface of the proposed BPF for 5.85 GHz, 30 GHz, 3 GHz, and 10 GHz are displayed in Fig.10. The red color regions designate the highest coupling, whereas the blue color regions indicate the lowest coupling. The maximum current can be observed at the passbands 5.85 GHz and 30 GHz which means that the coupling is the strongest, while the lowest current are at the stopbands 3 GHz and 10 GHz and hence, the coupling is the weakest. This demonstrates that low losses are present at the passbands and higher losses are in the stopbands due to the reflection of the power from the output the input port.

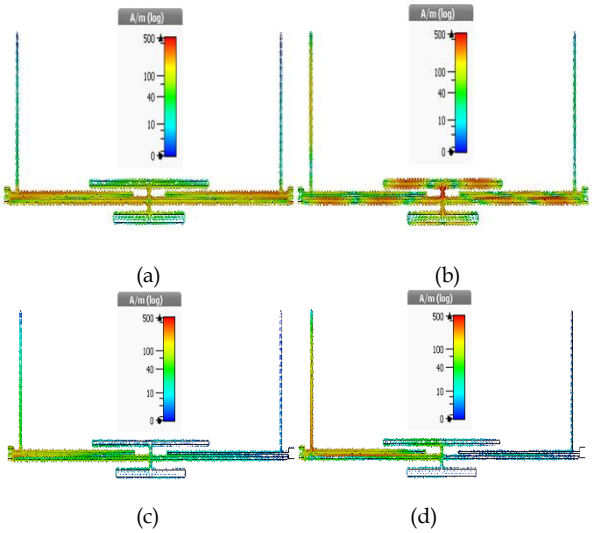

Fig.10. Surface current distribution at different frequencies: (a) 5.85GHz; (b) 30GHz; (c) 3GHz; (d) 10GHz.

5 COMPARISON WITH REPORTED BPFS

The dual-band BPF reports that have been previously issued are summarized in Table (3) and compared with the proposed BPF in terms of specification and performance to present the points that have been achieved in this work.

TABLE 3
COMPARISON BETWEEN REPORTED DUAL-BAND BPFS

Reference	f_0 (GHz)	IL (dB)	FBW (%)	Frequency ratio
[1]	2.45/5.4	0.9/0.9	25/15.1	2.2
[4]	2.45/5.2	0.6/0.9	18/4.8	2.12
[5]	0.61/1.36	0.45/0.75	32.3/10.5	2.23
[7]	2.475/3.49	1.2/1.2	15.6/8	1.41
[15]	2.37/29.84	0.75/1.74	19.41/6.5	12.59
This work	5.85/30	0.2/0.4	42.6/3.6	5.13

As can be seen in the table above, the proposed filter achieved the largest frequency ratio in comparison with [1] to [7] and less reflection. The filter in [15] has the largest frequency ratio but at the expense of circuit simplicity since the design is very complex with multi-layer materials, so this is considered as a disadvantage in terms of the design. This proposed filter is the simplest in design among all of the aforementioned filters.

6 CONCLUSIONS

In this paper, a compact and simple BPF is proposed by using a two parallel coupled microstrip lines and two T-shaped lines opposite to each other at the center of the filter with the insertion of two stubs at both side and defection at the ground for the sake of performance enhancement. Two passbands are achieved an ultra-wide rejection band between them. The high frequency ratio is achieved by multi-stubs have been used with the structure of the DGS. The two passbands are centered at 5.85 GHz for WLAN applications, and 30 GHz that can be used in high speed data transmission and 5G communication systems. The filter reveals good performance with the available simple and compact structure.

REFERENCES

[1] Lin-Chuan Tsai and Ching-Wen Hsue, "Dual-Band Bnadpass Filter Using Equal-Length Coupled-Serial-Shunted Lines and Z-Transform Technique," *IEEE Trans. on Microw. Theo. and Tech.*, vol. 52, No. 4, pp. 1111-1117, April 2004.

[2] Jin Xu, Wen Wu, and Chen Miao, "Compact Microstrip Dual-/Tri-/Quad-Band Bandpass Filter Using Open Stubs Loaded Shorted Stepped-Impedance Resonator," *IEEE Trans. on Microw. Theo. and Tech.*, vol. 61, No. 9, pp. 3189-3199, Sept. 2013.

[3] Wei Jiang, Wei Shen, Tengxing Wang, Yong Mao Huang, Yujita Peng, and Guoan Wang, "Compact Dual-Band Filter Using Open/Short Stub Loaded

Stepped Impedance Resonators (OSLSIRs/SSLSIRs) ," *IEEE Microw. and Wirel. Compon. Lett.*, vol. 26, No. 9, pp. 672-674, Sept. 2016.

[4] Xiu Yin Zhang, Jian-Xin Xhen, Quan Xue, and Si-Min Li, "Dual-Band Bandpass Filters Using Stub-Loaded Resonators," *IEEE Microw. and Wirel. Compon. Lett.*, vol. 17, No. 8, pp. 583-585, Aug. 2007.

[5] Nagendra Kumar and Yatendra Kumar Singh, "Compact stub-loaded open-loop BPF with enhanced stopband by introducing extra transmission zeros," *Electronic letters*, vol. 51, No. 2, pp. 164-166, Jan. 2015.

[6] Jin Shi, Longlong Lin, Jian-Xin Chen, Hui Chu, and Xu Wu, "Dual-Band Band-pass Filter With Wide Stopband Using One Stepped-Impedance Ring Resonator With Shorted Stubs," *IEEE Microw. and Wirel. Compon. Lett.*, vol. 24, No. 7, pp. 442-444, July 2014.

[7] Wenjie Feng; Quan Xue and Wenquan Che, "Compact dual-band bandpass filter based on stepped impedance resonators and T-shaped line," *Microw. and Optic. Tech. Lett.*, vol. 52, No. 4, pp. 2721-2724, Dec. 2010.

[8] Sheng Sun, "A Dual-Band Bandpass Filter Using a Sinlge Dual-Mode Ring Resonator," *IEEE Microw. and Wirel. Compon. Lett.*, vol. 21, No. 6, pp. 298-300, June 2011.

[9] Wei Qin and Quan Xue, "Complementary Compact Microstrip Resonant Cell and Its Applications to Microwave Single- and Dual-Band Bandpass Filters," *IEEE Trans. on Microw. Theo. and Tech.*, vol. 61, No. 2, pp. 773-781, Feb. 2013.

[10] Haiwen Liu, Baoping Ren, Xuehui Guan, Jiuhuai Lei and Shen Li, "Compact Dual-Band Bandpass Filter Using Quadruple-Mode Square Ring Loaded Resonator (SRLR) ," *IEEE Microw. and Wirel. Compon. Lett.*, vol. 23, No. 4, pp. 181-183, April 2013.

[11] Runqi Zhang and Lei Zhu, "Design of a compact dual-band bandpass filter using coupled stepped impedance resonators", *IEEE Microw. and Wirel. Compon. Lett.*, vol. 24, No. 3, pp. 155-157, March 2014.

[12] Yatao Peng, Lijun Zhang, Jun Fu, Yudong Wang and Yongqing Leng, "Compact Dual-Band Bandpass Filter Using Coupled Lines Multimode Resonator," *IEEE Microw. and Wirel. Compon. Lett.*, vol. 25, No. 4, pp. 235-237, April 2015.

[13] He Zhu and Amin M. Abbosh, "Single-and dual-band bandpass filters using coupled stepped-impedance resonators with embedded coupled-lines," *IEEE Microw. and Wirel. Compon. Lett.*, vol. 26, No. 9, pp. 675-677, Sept. 2016.

[14] Yang Xiong, Litian Wang, Doudou Pang, Wei Zhang, Fan Zhang, Ming He, Xinjie Zhao and Xu Zhang, "Dual-wideband bandpass filter with independently controllable center frequencies and wide stopband," *Intern. Journ. of Microw. and Wirel. Tech.*, vol. 10, No. 1, pp. 93-99, Feb. 2018.

[15] Shao Yong Zheng, Zhi Li Su, Yong Mei Pan, Zeeshan Qamar and Derek Ho, "New Dual-/Tri-Band Bandpass Filters and Diplexer With Large Frequency Ratio," *IEEE Trans. on Microw. Theo. and Tech.*, vol. 66, No. 6, pp. 2978-2992, June 2018.